ISSN: 2449 - 0539
BAYERO JOURNAL OF ENGINEERING AND TECHNOLOGY (BJET) VOL. 17 No. 3 AUGUST, 2022 PP 14-27

FABRICATION OF CARBON NANOTUBE-REINFORCED ALUMINIUM MATRIX COMPOSITE USING POWDER METALLURGY

Umma Abdullahi

Center for Energy Research and Training,
Ahmadu Bello University Zaria, P.M.B 1044 Samaru,
Post code: 810107 Kaduna State, Nigeria

Email: yabi78@yahoo.com*, ummaabdullahi@abu.edu.ng

ABSTRACT

Carbon nanotube reinforced Aluminium (CNT-Al) nanocomposites with four different concentrations of 1, 1.5, 2 and 2.5 wt% CNT were successfully fabricated using powder metallurgy route. Ball milling parameters such as preliminary mixing of CNT and Al in a tube via manual hand shaking and process control agent (PCA) were considered for the homogeneous and uniform dispersion of CNT in aluminium matrix with lower milling time. The characterization of CNT-Al mixed powder and CNT-Al nanocomposite were performed using SEM, FESEM, EDX and XRD analyzer. Density was measured using a digital densitometer and compared with the theoretical relative density. It was found that, 1 wt% CNT has the highest percentage of the relative density of 8.40%, Whilst 1.5 and 2 wt% showed almost same value for the relative density (≈77%), however, 2.5 wt% CNT in nanocomposite showed a slightly lower relative density of 74% indicating more lighter than 1.5 and 2 wt% CNT composition.The morphology of the developed CNT-Al nanocomposite showed uniform and homogeneous dispersion of CNT in the Al matrix. And 1.5 wt% CNT was assumed to have better and uniform CNT dispersion and it was achieved within short time of 250 and 300 rpm milling speed. Uniform and homogeneously dispersed CNT has a significant effect in reducing the weight of Al which lead to the achievement of the light weight CNT-Al nanocomposite.

1.0 INTRODUCTION

Composite materials are multiple phase materials achieved from non-natural mixture of dissimilar materials in order to get properties that the individual component by themselves cannot obtain and different phases are formed naturally by reactions, phase transformations, or other phenomena (Chung, 2010). Composite materials can be modified for a variety of properties by suitably choosing proportions, distributions, and morphologies, degrees of crystallinity, crystallographic textures, as well as the structure and composition of the interface between components. Therefore, composite materials can be designed to suit the needs of technologies relating to the aerospace, automobile, electronics, construction, energy, biomedical and other applications (Chung, 2010; Ajayan, Schadler and Braun, 2005). As a result, composite materials comprise most commercial engineering materials in the engineering applications.

The main benefits that composite components offer are reduced weight and assembly simplification. Furthermore, composites differ from traditional materials in that composite comprises two distinctly different components, reinforcement/filler and a matrix; a matrix can be polymeric, ceramic or metallic material (most often a polymer resin) that, when combined, remain discrete but function interactively to make a new material whose properties cannot be predicted by simply summing the properties of its components (Bradley et al., 2007).

A nanocomposite material has advantage of high surface to volume ratio of the reinforcing phase and/or its exceptionally high aspect ratio compared to the conventional composite materials (Bakshi, & Agarwal, 2011). The reinforcing material can be made up of particles, sheets or fibres. The area of the interface between the matrix and reinforcement phase is

typically an order of magnitude greater than for conventional composite materials.
Many researchers reported that a relatively small amount of nanoscale reinforcement can have a notable effect on the macroscale properties of the composite due to the large amount of reinforcement surface area (Noguchi, Magario, Fukazawa, Shimizu, Beppu, & Seki, 2004; Morsi, and Esawi, 2007; Esawi, Morsi, Sayed, Gawad, & Borah, 2009). For example, reinforcement of carbon nanotubes in to the metal matrix enhanced the thermal conductivity and electrical properties, heat resistance or mechanical properties such as stiffness, strength and resistance to wear and damage.
The materials used as a matrix in metal matrix composites (MMCs) are usually Aluminium, magnesium, copper, titanium, Al-lithium, and super alloys (Bakshi, Lahiri, & Agarwal, 2010). According to many researchers, Al-based (MMC) are widely used composite materials due to their relatively low density, high specific stiffness, and wear resistance. MMC's can be developed by dispersing reinforcing materials that have unique physical properties such as oxides, carbides or nitrides in the Al matrix (Bakshi and Agarwal, 2010). The composite carries the applied load by transferring it from the matrix to the reinforcement. The produced composite will have combined properties of its constituting elements, and this is the main reason behind the development and success of MMC manufacturing since the type and amount of the constituents of the composite could easily be altered to obtain the desired properties of the new product (Ci, Ryu, Jin-Phillipp, &Rühle, 2006; Edtmaier, Janhsen, Hula, Pambaguian, Wulz, Forero, Stefan Hepp, 2009; Schadler, Giannaris, & Ajayan, 1998).
Al matrix composites have wide prospects of application in aviation, spaceflight and automobile due to lower density which is one of the requirements necessary for the weight reduction for many components in order to save fuels and hence energy (Surappa, 2003).

Powder metallurgy (PM) is considered to be the most common and reliable production technique for nanocomposite fabrication, which can be characterized by high quality dimensional and geometrical precision as well as good mechanical properties (Bui, Tran, Le, Than, Doan, Phan, 2011). Using PM process, several properties of metal matrix nanocomposite can be achieved, such as increased in hardness, wear resistance, mechanical and thermal durability, and thermal conductivity but decreases the density of the material.Powder metallurgy route is sub divided in to four different steps depending on the approach. The basic process steps consist of preparation of raw materials in powder form, blending and mixing of the raw materials as matrix and reinforcement (also known as pre-compaction activities) followed by compaction and finally sintering with additional treatments (DeGarmo, Canada, Sullivan, 1979). Figure 1.0 shows a typical process step for powder metallurgy route.

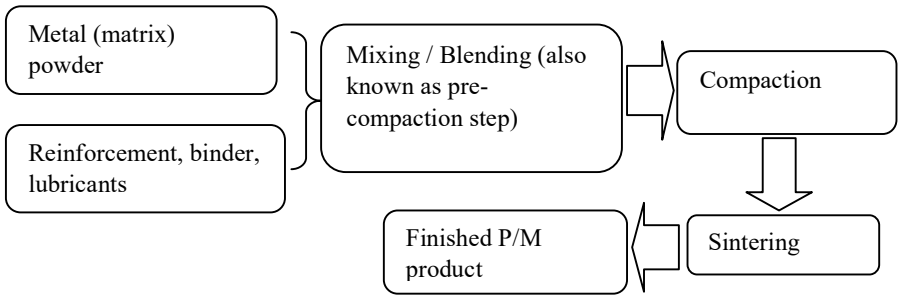

Figure 1.0: Typical powder metallurgy process steps

In general, any method adopted for the nano reinforcement, uniform and homogeneous dispersion of the nano materials into the matrix should be ensured before achieving the targeted properties of the nanocomposite material (Tolochko, Klimova, Ordanian, Cheong, & Kim, 2009). The percentage by weight (*mass fraction*) of the nanoparticulates introduced can remain very low (on the order of 0.5% to 5%) due to the fact that small addition of the reinforcement material can enhance the properties of the

matrix materials and there is a low flow ability of such materials in to the matrix, especially for the most commonly used non spherical, high aspect ratio fillers (e.g. nanometer thin platelets, such as clays, or nanometer diameter cylinders, such as carbon nanotubes). The main aim of this paper is to develop carbon nanotube reinforced Aluminium (CNT-Al) nano-composite using powder metallurgy route.

2.0 MATERIAL AND METHODS

The experiment started with the preparation and characterization of both reinforcement and matrix materials. The four weight percentage of CNTs such as 1, 1.5, 2.0 and 2.5 wt %, were selected as reinforcement inpure Al as a matrix. The carbon nanotube reinforced aluminium matrix composite (CNT-AMC) mixture were pre-mixed via manual hand shake in a tube together with some milling ball in a ball to powder ratio (BPR) of 5:1 for about 20 minutes and then blended using ball mill machine with different milling time. The mixed and blended powders were compacted using unidirectional hydraulic press carver cold press compaction machine at a suitable pressure of 17 and 52 MPa based on the quantity of the composite powder. The compacted sample was sintered using hot isostatic press (HIP) machine (HP630) at 500 ^{o}C temperature for 60 min with the supply of argon gas to the system at a released pressure of 17 MPa at 30 seconds interval throughout the process to control the sintering condition. JEOL, JSM 5600 scanning electron microscope (SEM) at 15 kV working voltage with 33 mm working distance and JEOL, JSM 67OOF field emission scanning electron microscope (FESEM) at 10 kV working voltage and 7-8.5 mm working distance were used to characterize the as received Al, CNT and CNT-Al mixed composite powders. The fabricated CNT-Al nanocomposite was analyzed using FESEM integrated with EX-23000BU energy dispersive X-ray analyser (EDX) at 10 kV working voltage and 0.1 mA current.The physical properties were determined by measuring the densities of the compacted composites and comparing them to the theoretical density. Table 2.0 presents the composition of the raw materials with appropriate quantity of ethanol as process control agent.

Table 1.0Specifications of raw materials (CNT and Al) for this research work

Material	Specification	Value
CNT	Purity (%)	> 98
	Average diameter (nm)	10-11
	Average length (μm)	5-15
	Surface area (m^2g^{-1})	230-280
	Aspect ratio, *l/D*	≈ 952
Al	Purity (%)	99.7
	Average particle size (μm)	78
	Sub-particles (μm)	20-30

Figure 2.0: Tungsten carbide milling balls of 10 mm diameter with the average weight of 7g delete noimportant

Table 2.0 Mixing composition of CNT-Al nanocomposite

Sample	Composition of nanocomposite (wt %)	Abbreviation?
1	Al (99) + CNT (1.0) + Ethanol (1.0 ml)	1 wt%
2	Al (98.5) + CNT (1.5) + Ethanol (1.0 ml)	1.5 wt %
3	Al (98.0) + CNT (2.0) + Ethanol (0.85 ml)	2.0 wt %
4	Al (97.5) + CNT (2.5) + Ethanol (0.85)	2.5wt %

Figure 3.0: Ball milling operation set up using argon gas

Figure 4.0 shows a flow diagram of the sintering process which was employed in this research work. In this investigation, the sample was sintered using hot isostatic press (HIP) machine (HP630) at 500 ^{o}C and the argon gas was supplied at a pressure of 17 MPa and was heated for a period of 60 min at a controlled atmosphere. The sintering chamber was then slowly cooled and depressurized to remove the sample safely. Figure 5.0 shows the experimental set up for HIP sintering. The feature of HIP sintering process is that all the expected internal porosity in the green compact can be closed without distorting external geometry, in addition powder materials will be strengthened to almost the theoretical density through perfect diffusion bonds between CNT and Al powders. The CNT-Al sintered part was removed from the ceramic sample container after the sintering process and was subjected to successive operations.

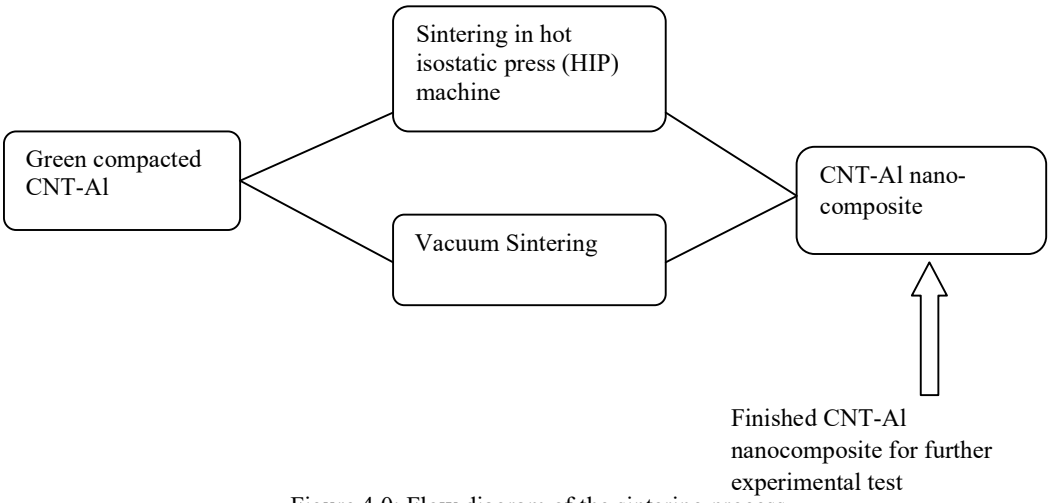

Figure 4.0: Flow diagram of the sintering process

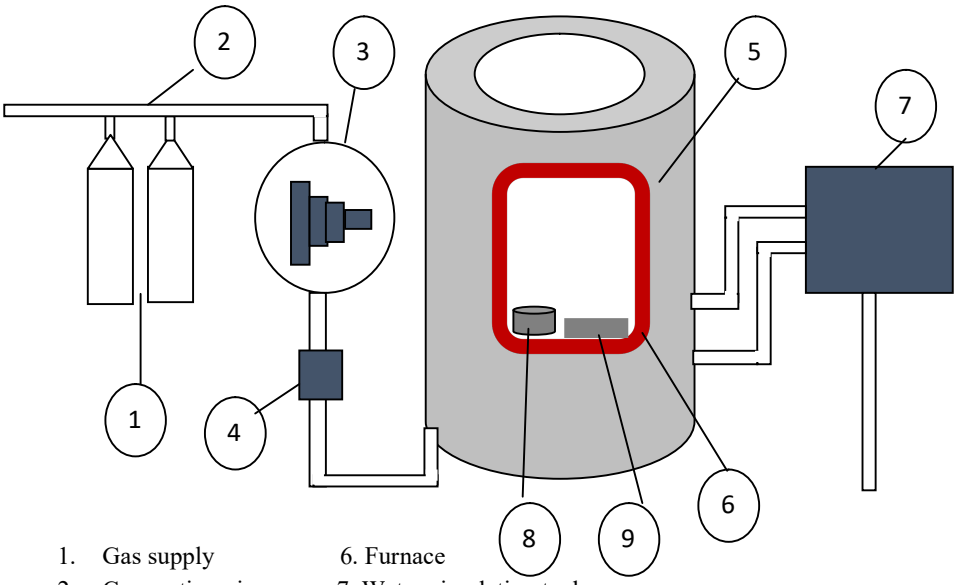

1. Gas supply
2. Connecting pipe
3. Compressor
4. Filter chamber
5. Mantle heat shield
6. Furnace
7. Water circulation tank
8. Circular CNT-Al green compact
9. Rectangular CNT-Al green compact

Figure 5.0: Experimental set-up of hot isostatic press sintering

3.0 RESULTS AND DISCUSSIONS

3.1 Characterisation of Raw Materials

In this investigation, field emission scanning electron microscope (FESEM) was employed for the characterization of CNT powder. Scanning electron microscope (SEM) was used to characterize the aluminium (Al) powder.

3.1.1 Characterisation of CNT Powder

Figure 6.0 presents the image of CNT powder at lower and higher magnifications. Carbon nanotube appears like sponge in mass when observed under FESEM at lower magnification.

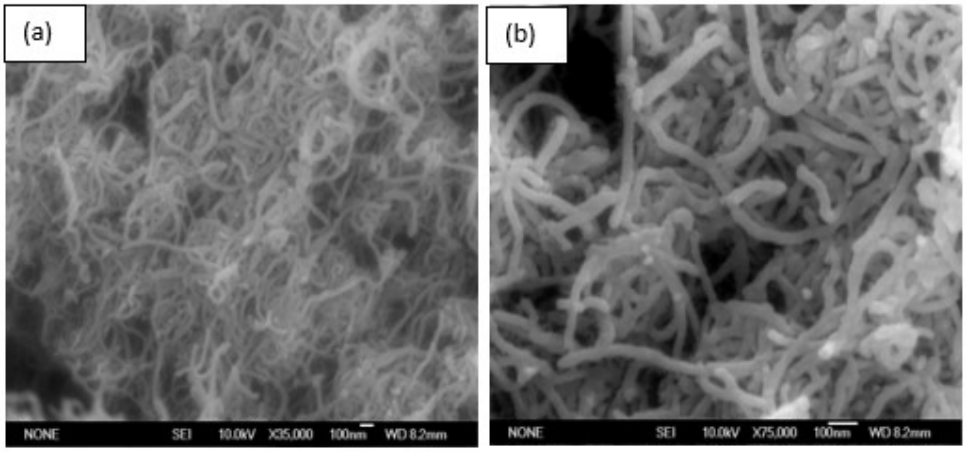

Figure 6.0: FESEM image of CNT powders at: (a) X35, 000 magnification and (b) X75, 000 magnifications.

The sponge like nature of appearance of CNT in mass at lower magnification makes it necessary to employ higher magnification value to clearly observe and study the morphology and the structure appropriately. From the FESEM image at higher magnification, the CNT was observed to be a long and thin tube-like structure and appeared as individual molecules as expected, which leads to further study of the structure. Figure 7.0 is the EDX analysis result of the CNT powders. The carbon peak was detected for the CNT powder from EDX analyser. From the spectrum, it was observed that there is no impurity in the powders as indicated by only one peak of carbon.

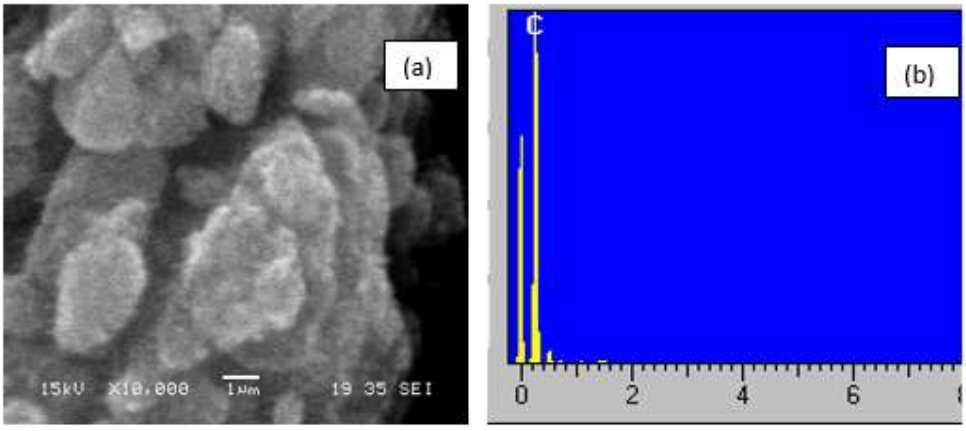

Figure 7.0: (a) SEM image and (b) EDX spectrum of CNT powders

3.1.2 Characterisation of Al powder

Aluminium powder was characterized using SEM and EDX analyser. Figure 8.0 presents the image of Al powders along with the EDX spectrum. SEM image of pure Al showed large nearly spherical silvery structures with a satellite of fine sub particles which were observed at two different magnifications (Fig. 8.0). It has a size range of approximately 75-78 μm. From the observed elemental peaks (Fig. 8.0c) it is found that the used aluminium was 99.7% pure with

0.31% Fe as impurities. There is a small elemental peak of carbon observed which is as a result of the carbon tape used to mount the Al powders on to the sample holder. The effect of the impurity materials was not significant, hence, would not have any effect on the property of Al.

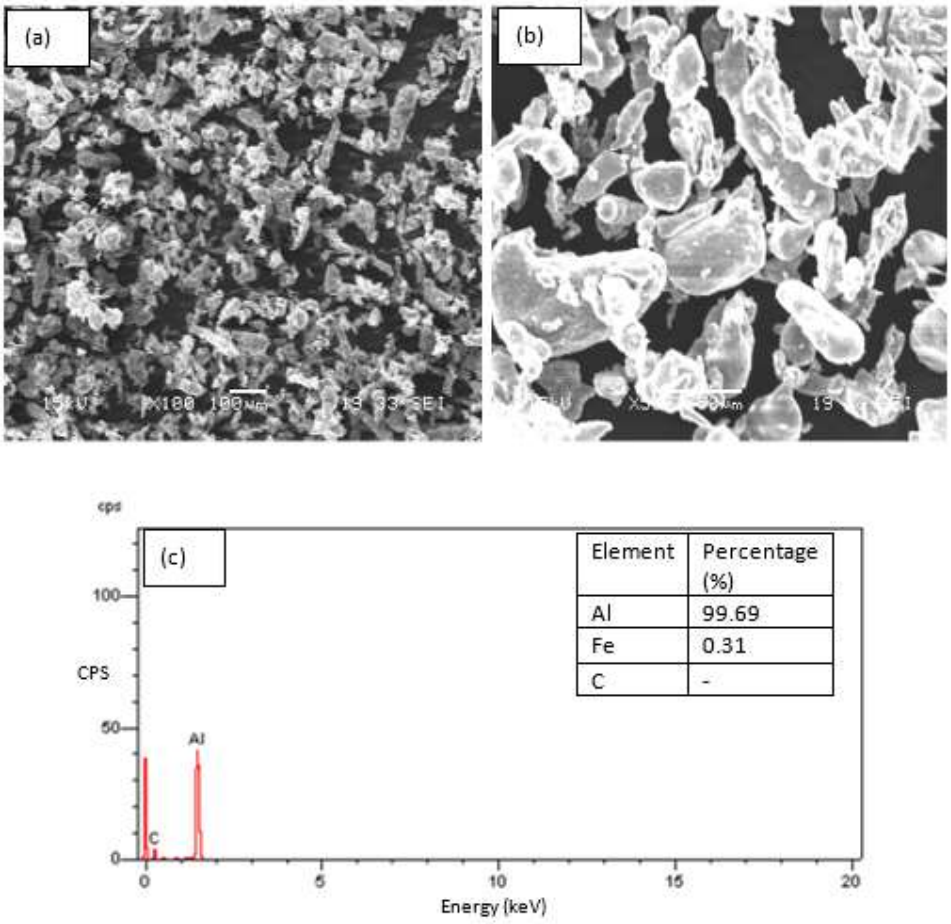

Figure 8.0: SEM and EDX analysis of Al powders (a) X100 magnification, (b) X300 magnifications and (c) EDX spectrum

3.2 Characterization of the ball milled CNT-Al powders

In the milling process the ball has impact on the Al powder particles which caused a severe plastic deformation of the powder. . As a result of that, plastic deformation at high strain rates takes place within the Al particles and most of the energy in a form of mechanical energy in the deformation course of action is transformed to heat and little of it remains in the particles, thus raising the inner energy (Lynch, & Rowland, 2005). Al particles experience changes in shape and size during ball mill operation as a result of the impact.

3.2.1 Morphology of CNT-Al nano-composite

The sintered CNT-Al nanocomposite was ground to study the morphology and the CNT dispersion in to the Al matrix. Figs. 9.0-12.0 shows the FESEM micrograph of 1, 1.5, 2 and 2.5 wt% CNT-Al nanocomposites milled at 250 rpm for 2hrs after HIP sintering at 500 ^{o}C for 60 min in an argon gas atmosphere. The morphological view from these figures showed the uniform dispersion of CNT into the Al and existence of good bonding of CNT at the surface of Al particles in the nanocomposite. These higher magnification FESEM analysis micrographs presentedshowed the presence of CNT within the matrix on the developed CNT-Al nanocomposite after sintering. Deformed and cracked particles of Al show the embedded individual CNT on the surface of Al matrix. It was observed that the

CNT remained undamaged after mechanical alloying under desired milling conditions.

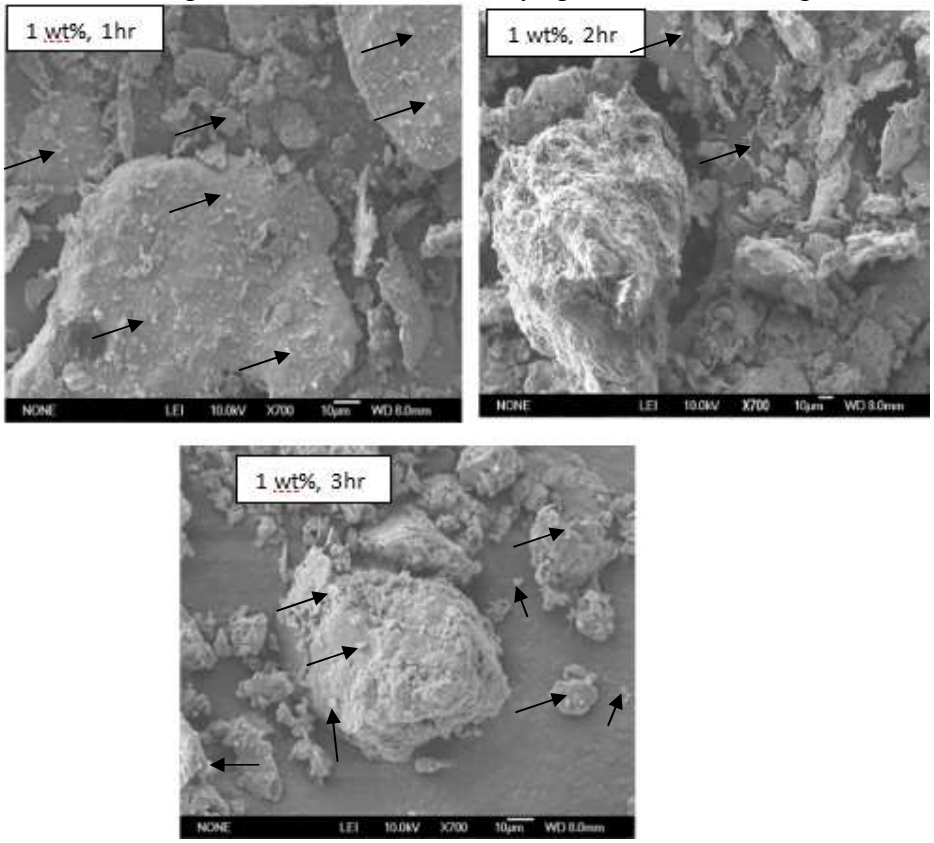

Figure 9.0: FESEM micrographs showing the embedded individual CNT on the surface of Al matrix and morphology for 1 wt% CNT at 250 rpm

Morsi and Esawi (2007) used powder metallurgy to study the effect of mechanical alloying time and carbon nano tube content on the evolution of Al-CNT composite powders for 48 hrs of milling time and 200 rpm speed and they achieved homogenization of CNT in aluminium at that milling time and 200 rpm speed. In their study, homogenization of CNT in aluminium with the round smooth surface occurs only for 2 wt% CNT. Whilst, in this investigation, no much difference was observed regarding the transformation occurred in terms of shape and morphology of the mixed and blended CNT-Al powders for both CNT contents at the two different milling speeds used.

In terms of homogenization 1.5 wt% CNT was assumed to have better and uniform CNT dispersion and it was achieved within short time of 250 and 300 rpm milling speed. Higher CNT percentage into Al matrix demanded more milling time to homogeneously dispersed CNT in to the Al matrix than lower CNT percentage mixture. Uniform and homogeneously dispersed CNT has a significant effect in a light weight CNT-Al nanocomposite. Hence, it can be said that, the milling time was reduced significantly for the dispersion and homogenization of CNT into the Al matrix, and it can be postulated that slight CNTs percentage variations, the use of appropriate quantity of PCA and the preliminary mixing of CNTs and aluminium powder in a tube via manual shaking could be the main contributing factor in achieving uniform dispersion of CNT in Al matrix.

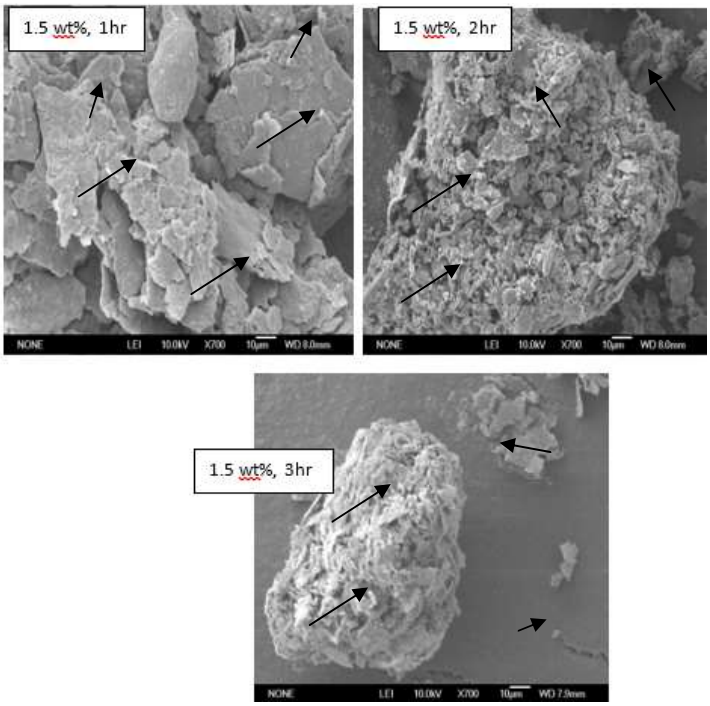

Figure 10.0: FESEM micrographs showing the embedded individual CNT on the surface of Al matrix and morphology for 1.5wt% CNT at 250 rpm

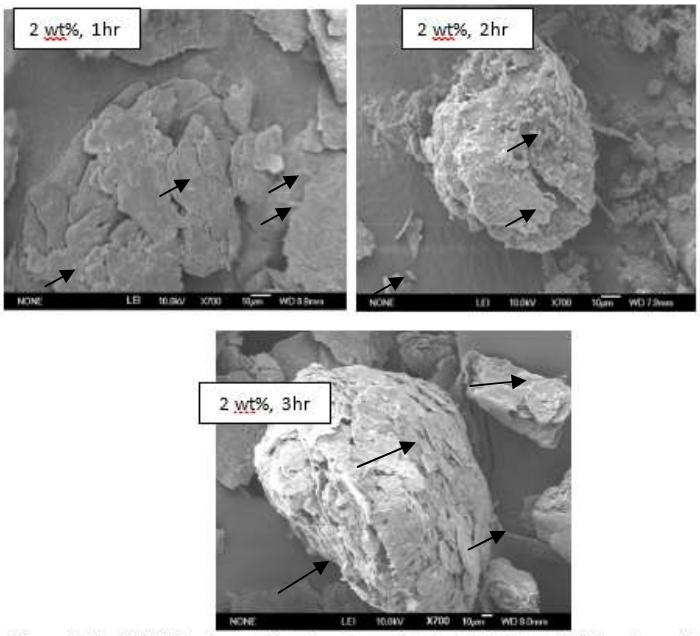

Figure 11.0: FESEM micrographs showing embedded individual CNT on the surface of Al matrix and morphology for 2 wt% CNT at 250 rpm

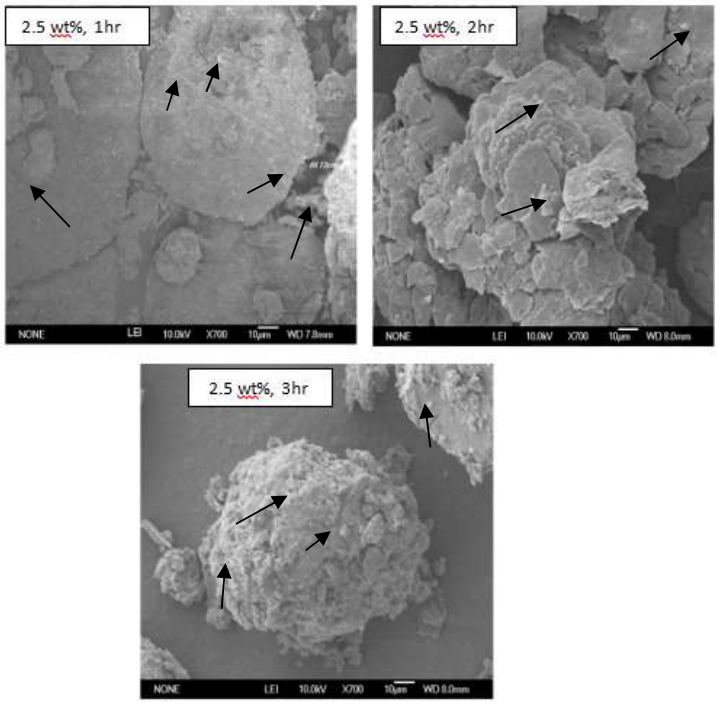

Figure 12.0: FESEM micrographs showing the embedded individual CNT on the surface of Al matrix and morphology for 2.5 wt% CNT at 250 rpm

3.3 Effect of sintering on CNT-Al nanocomposite

Effects of sintering on the physical properties such as measured mass and relative density of CNT-Al nanocomposite were plotted against the milling time and shown in Figs. 13.0 and 14.0. At the initial stage, the weight of each sample was measured before and after sintering at HIP machine. Figure 13.0 shows the measured mass with respect to milling time for all the four compositions of the nano-composite before and after sintering. For all the compositions of CNT-Al nanocomposite similar trend was observed with the mass of CNT-Al nano-composite sample in air doubled its mass in liquid.

However, the mass decreased with almost 55% of the measured value after HIP sintering at 500 ^{o}C, which was due to the evaporation of the PCA during processing of the CNT-Al nanocomposite and the effect of sintering mechanism on the particles (densification). From Fig. 4.22 it showed that at the initial hour of milling there was a variation of mass for the four CNT compositions with 1.5 wt% showed the highest mass followed by 1 and 2 wt% CNT. 2.5 wt % showed the lowest mass before sintering at the first hour of milling. The mass decreased for all the CNT composition with almost the same percentage after sintering. At the second hour of milling all the four CNT wt% showed almost the same level of mass before sintering with almost the same level also after sintering that was roughly 55% lower the mass before sintering. The density of CNT-Al nanocomposite after HIP sintering was measured and compared with the theoretical density of the material. Figure 14.0 shows the plot of the relative density (RD) of the developed CNT-Al nanocomposites against the milling time for 1, 1.5, 2 and 2.5 wt% CNT. It was found that density decreased with increasing milling time for all CNT composition with the highest density for the green compact nano-composite powder milled for 2 hr for 1, 1.5 and 2 wt% CNT.

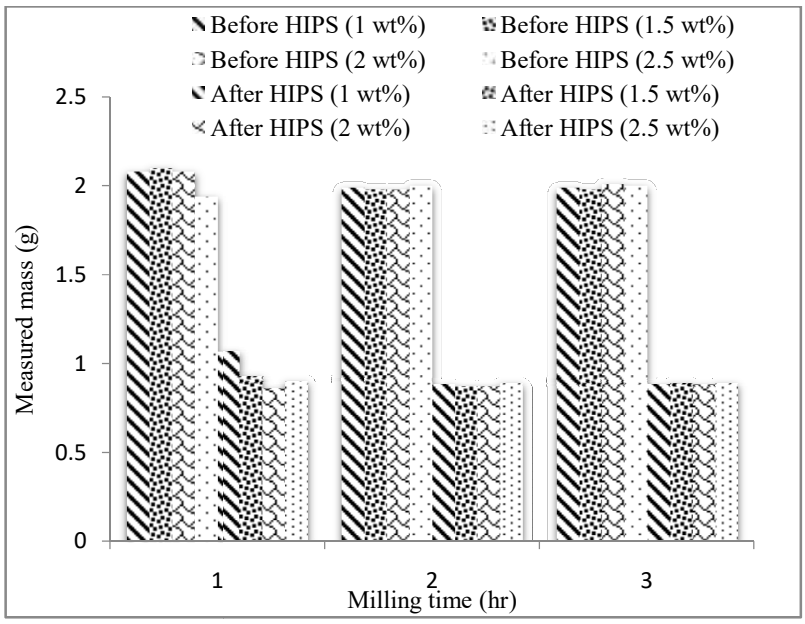

Figure 13.0: Measured mass (g) of developed CNT-Al nanocomposite before and after sintering plotted against the milling time for 1, 1.5, 2 and 2.5 wt% CNT

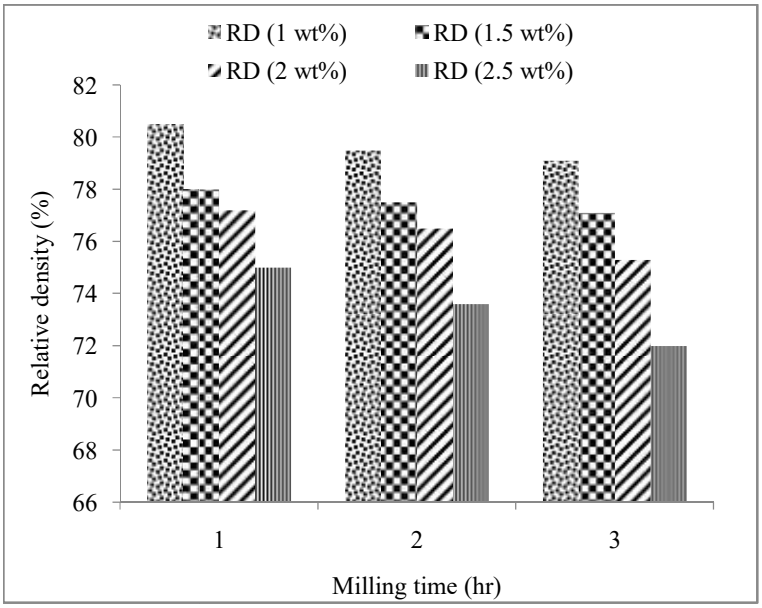

Figure 14.0: Relative density (bulk density/theoretical density) of CNT-Al nanocomposite after HIP sintering at 500 ^{o}C for 60 min plotted against the milling time for 1, 1.5, 2 and 2.5 wt% CNT

Whereas, for 2.5 wt% CNT the density was higher from the initial hour and decreased slightly at the 2 hr and 3 hr of milling. From the data, it is indicated that 1 wt% CNT has the highest percentage of the relative density of 80.4%, which might be as a result of the highest ductility that is close to that of pure Al and the little porosity due to the lower CNT content. Whilst 1.5 and 2 wt% showed almost same value for the relative density (76.7%), however, 2.5

wt% CNT in nanocomposite showed a slightly lower relative density of almost 74% indicating more lighter than 1.5 and 2 wt% CNT composition. The variation of the relative density was mainly due to processing and the slight difference in the CNT content in the nanocomposite and the higher the CNT percentage the less dense the material.

From the experimental results, highest density was observed with the nanocomposite samples of powder milled for 2 hr for 2 and 2.5 wt%, whilst, for 1 and 1.5 wt% the highest density was at the initial hour. This was due to the less homogeneous mixture of CNT and the Al in 2 and 2.5 wt% CNT and higher CNT percentage may result in much cluster and agglomeration of CNT. The Al weight was because there is no effect of CNT on Al matrix in higher percentage of CNT in the composite. As the milling continue the CNT dispersed uniformly and it showed a significant effect on the mass of Al matrix for making it lighter. Whilst, in the case of 1 and 1.5 wt% the CNT percentage is smaller and it quickly dispersed uniformly even from the initial hour making the mixture lighter due to the CNT effect on to the Al matrix. In contrast the densities of the sintered samples without argon gas were higher than that sintered with argon gas using HIP machine, this was because CNT may react with aluminium to form carbide compounds such as Al_4C_3 which may increase the density of the material. It can be said that, properly controlled atmosphere can prevent the reaction at high temperature which may prevent the material from getting additional weight from the unwanted materials such as carbide.

4.0 CONCLUSION

CNT-Al nanocomposites with four different concentrations of 1, 1.5, 2 and 2.5 wt% CNT were successfully developed using powder metallurgy route. It was found that, 1 wt% CNT has the highest percentage of the relative density of ≈80%, Whilst 1.5 and 2 wt% showed almost same value for the relative density (≈77%), however, 2.5 wt% CNT in nanocomposite showed a slightly lower relative density of almost 74% indicating more lighter than 1.5 and 2 wt% CNT composition. From the morphology of the developed CNT-Al nanocomposite which showed uniform and homogeneous dispersion of CNT in to Al matrix (Fig. 9-12), it was deduced that powder metallurgy route is the most economical and effective method of developing CNT-Al nano-composite with non-destructive features.

5.0 REFERENCES

Adebisi, A. A., Maleque, M., & Rahman, M. (2011). Metal matrix composite brake rotor: Historical development and product life cycle analysis. *International Journal of Automotive and Mechanical Engineering (IJAME), 4*, 471-480.

Adler, D. (2008). Mercedes-Benz. MBI Publishing. p. 167. ISBN 978-0-7603-3372-3. Retrieved, 2010-11-11.

Ajayan, P. M., Schadler, L. S., & Braun, P. (2005). Nanocomposite science and technology 2003: Wiley-VCH Verlag, Weinheim.

Aji, I., Sapuan, S., Zainudin, E., & Abdan, K. (2009). Kenaf fibres as reinforcement for polymeric composites: a review. *International Journal of Mechanical and Materials Engineering, 4*(3), 239-248.

Allison, J. E., & Cole, G. S. (1993). Metal-matrix composites in the automotive industry: opportunities and challenges. *JOM Journal of the Minerals, Metals and Materials Society, 45*(1), 19-24.

Esawi, A. M., Morsi, K., Sayed, A., Gawad, A. A., & Borah, P. (2009). Fabrication and properties of dispersed carbon nanotube–aluminium strips. *Composites Science and Technology, 68*(2), 486-492.

aluminum composites. *Materials Science and Engineering: A, 508*(1), 167-173.

Hansang Kwon, D. H. P., Jean François Silvain, Akira Kawasaki (2010). Investigation of carbon nanotube reinforced aluminum matrix composite materials. [Short communication]. *composites Science and Technology, 70*, 546–550.

He, C., Zhao, N., Shi, C., Du, X., Li, J., Li, H., et al. (2007). An approach to obtaining homogeneously dispersed carbon nanotubes in Al powders for preparing reinforced al-matrix composites. *Advanced Materials, 19*(8), 1128-1132.

Iijima, S. (1991). Helical microtubules of graphitic carbon. *Nature, 354*(6348), 56-58.

Javadi, A., Mirdamadi, S., Faghihisani, M., Shakhesi, S., & Soltani, R. (2012). Fabrication of well-dispersed, multiwalled carbon nanotubes-reinforced aluminum matrix composites. *New Carbon Materials, 27*(3), 161-165.

Jiang, L., Li, Z., Fan, G., Cao, L., & Zhang, D. (2012). The use of flake powder metallurgy to produce carbon nanotube (CNT)/aluminum composites with a homogenous CNT distribution. *Carbon*, 50, 1993-1998.

Kannan, S., & Kishawy, H. (2008). Tribological aspects of machining aluminium metal matrix composites. *Journal of Materials Processing Technology, 198*(1), 399-406.

Kim, K. T., Lee, K. H., Cha, S. I., Mo, C.-B., & Hong, S. H. (2004). Characterization of carbon nanotubes/Cu nanocomposites processed by using nano-sized Cu powders.*Paper presented at the Mater Soc Symp Proc.*

Kwon, H., Park, D. H., Silvain, J. F., & Kawasaki, A. (2010). Investigation of carbon nanotube reinforced aluminum matrix composite materials. *Composites Science and Technology, 70*(3), 546-550.

Lai, S. W., & Chung, D. (1994). Fabrication of particulate aluminium-matrix composites by liquid metal infiltration. *Journal of Materials Science, 29*(12), 3128-3150.

Langworth, R. M. (The Post war Years, 1994). Chrysler and Imperial: *Motor books international.* ISBN 0-87938-034-9.

Lawrence, M. (1991). *A to Z of sports cars, Bay view books. ISBN 978-1-870979-81-8.*

Li, H., Misra, A., Zhu, Y., Horita, Z., Koch, C. C., & Holesinger, T. G. (2009). Processing and characterization of nanostructured Cu-carbon nanotube composites. *Materials Science and Engineering: A, 523*(1), 60-64.

Liao, J. Z, Tan, M. J, & Sridhar, I. (2010). Spark plasma sintered multi-wall carbon nanotube reinforced aluminum matrix composites. *Materials & Design, 31*, S96-S100.

Liao, J., & Tan, M. J. (2011). Mixing of carbon nanotubes (CNTs) and aluminum powder for powder metallurgy use. *Powder Technology, 208*(1), 42-48.

Liao, J. Z., Tan, M. J., Ramanujan, R. V., & Shukla, S. (2011). Carbon nanotube evolution in aluminum matrix during composite fabrication process.*Paper presented at the Materials Science Forum.*

Lim, D., Shibayanagi, T., & Gerlich, A. (2009). Synthesis of multi-walled CNT reinforced aluminium alloy composite via friction stir processing. *Materials Science and Engineering: A, 507*(1), 194-199.

Poirier, D., Gauvin, R., & Drew, R. A. (2009). Structural characterization of a mechanically milled carbon nanotube/aluminum mixture. *Composites Part A: Applied Science and Manufacturing, 40*(9), 1482-1489.

Salimi, S., Izadi, H., & Gerlich, A. (2011). Fabrication of an aluminum–carbon nanotube metal matrix composite by accumulative roll-bonding. *Journal of Materials Science, 46*(2), 409-415.

Sannino, A., & Rack, H. (1995). Dry sliding wear of discontinuously reinforced aluminum composites: review and discussion. *Wear, 189*(1), 1-19.

Schadler, L., Giannaris, S., & Ajayan, P. (1998). Load transfer in carbon nanotube epoxy composites. *Applied Physics Letters, 73*, 3842.

Shaffer, J., Philippidis, T. P., & Vassilopoulos, A. P. (2004). 1. A Polymer Composites 1.1 Description. *The Handbook of Advanced Materials: Enabling New Designs*, 1.

Singhal, S., Pasricha, R., Teotia, S., Kumar, G., & Mathur, R. (2011). Fabrication and characterization of Al-matrix composites reinforced with amino-functionalized carbon nanotubes. *Composites Science and Technology*, 72, 103-111.

Surappa, M. (2003). Aluminium matrix composites: Challenges and opportunities. *Sadhana, 28*(1), 319-334.

Suryanarayana, C. (2001). Mechanical alloying and milling. *Progress in Materials Science, 46*(1), 1-184.

Suryanarayana, C., Ivanov, E., & Boldyrev, V. (2001). The science and technology of mechanical alloying. *Materials Science and Engineering: A, 304*, 151-158.

Xu, L.-S., Chen, X.-h., Wu, Y.-r., Pan, W.-Y., Xu, H.-y., & Zhang, H. (2006). Preparation of CNTs/Cu composite. *Chinese Journal of Nonferrous Metals, 16*(3), 406.

Yazdanbakhsh, A., Grasley, Z., Tyson, B., & Abu Al-Rub, R. K. (2011). Dispersion quantification of inclusions in composites. *Composites Part A: Applied Science and Manufacturing, 42*(1), 75-83.

Yourdkhani, M., & Hubert, P. (2012). Quantitative Dispersion Analysis of Inclusions in Polymer Composites. *ACS applied materials & interfaces, 5*(1), 35-41.

Zare, H., Toroghinejad, M. R., & Meratian, M. Dispersion of multiwalled carbon nanotubes in aluminum powders with ultrasonic and ball mill attrition. Paper presented at the *International Conference on Mechanical, Automotive and Materials Engineering (ICMAME'2012). Dubai, Jan. 7-8, 2012*

Zhao, N., Nash, P., & Yang, X. (2005). The effect of mechanical alloying on SiC distribution and the properties of 6061 aluminum composite. *Journal of Materials Processing Technology, 170*(3), 586-592.

Zulfia, A., Atkinson, H., Jones, H., & King, S. (1999). Effect of hot isostatic pressing on cast A357 aluminium alloy with and without SiC particle reinforcement. *Journal of Materials Science, 34*(17), 4305-4310.